Biochemistry

 Volume 37, Number 3 January 20, 1998

Accelerated Publications

Alternative Modes of Substrate Distortion in Enzyme and Antibody Catalyzed Ferrochelation Reactions†

Milton E. Blackwood, Jr.,‡ Thomas S. Rush III,‡ Floyd Romesberg,§ Peter G. Schultz,§ and Thomas G. Spiro*,‡

Department of Chemistry, Princeton University, Princeton, New Jersey 08544, and The Howard Hughes Medical Institute, Department of Chemistry, University of California, Berkeley, California 94720

Received October 22, 1997; Revised Manuscript Received December 8, 1997

ABSTRACT: Both an antibody that catalyzes metal insertion into porphyrins and the corresponding enzyme, ferrochelatase, are shown by resonance Raman spectroscopy to induce distortion in the bound porphyrin substrate. It was found that the enzyme-induced distortion is different from that induced by the antibody; the catalytic antibody produces a distortion which is similar to the one present in the hapten, *N*-methylmesoporphyrin IX (N-MeMP). Activation of specific out-of-plane vibrational modes reveal that the antibody induces an alternating up-and-down tilting of the pyrrole rings, while ferrochelatase induces tilting of all four pyrrole rings in the same direction (doming). Both distortions are effective in catalyzing metal insertion. The distortion induced in the enzyme is only seen when an inhibitory metal ion is also bound. This observation suggests an allosteric mechanism, in which a conformational change which distorts the porphyrin toward the transition state geometry, is induced by metal binding at an adjacent site. In contrast, the antibody does not have a metal binding site and appears to function largely through binding interactions with the porphyrin.

The concept of Haldane and Pauling (*1*) that enzymes catalyze reactions by binding more tightly to the transition state than to the reactants or products has been profoundly useful in probing the chemical mechanisms of enzymes, as well as designing new ones (*2*). The recent development of catalytic antibodies depends heavily on this concept (*3*). A stable molecule, which models the transition state of a reaction, is used as a hapten to elicit antibodies with complementary binding sites. If the hapten closely resembles the transition state, the antibody will catalyze the reaction. This strategy has produced a wide variety of catalytic antibodies, many with impressive catalytic power (*3*).

A comparison between the mechanism of an antibody-catalyzed reaction and that of the corresponding enzyme can provide insights into the chemical requirements of the reaction. Here we show spectroscopically that both an antibody and an enzyme which catalyze the insertion of metal ions into porphyrins induce distortion or strain in their bound substrates, evidence of an active site whose structure is more complementary to that of the transition state than substrate. However, the enzyme and antibody induce different distortions in the porphyrin. This indicates that the protein uses different binding interactions to affect the same chemical transformation, much like the serine and aspartyl proteases. The distortion induced by the antibody, an up/down tilt of the pyrrole rings, is similar to that programmed into the structure of the N-alkylporphyrin hapten. On the other hand, the enzyme induces a doming of the porphyrin ring which occurs upon binding of metal ion. Several other occurrences

† This work was supported by a grant from the National Institute of General Medical Science of the National Institutes of Health (GM 33576).

* Author to whom correspondence should be addressed.
‡ Princeton University.
§ University of California.

S0006-2960(97)02616-0 CCC: $15.00
Published on Web 01/06/1998

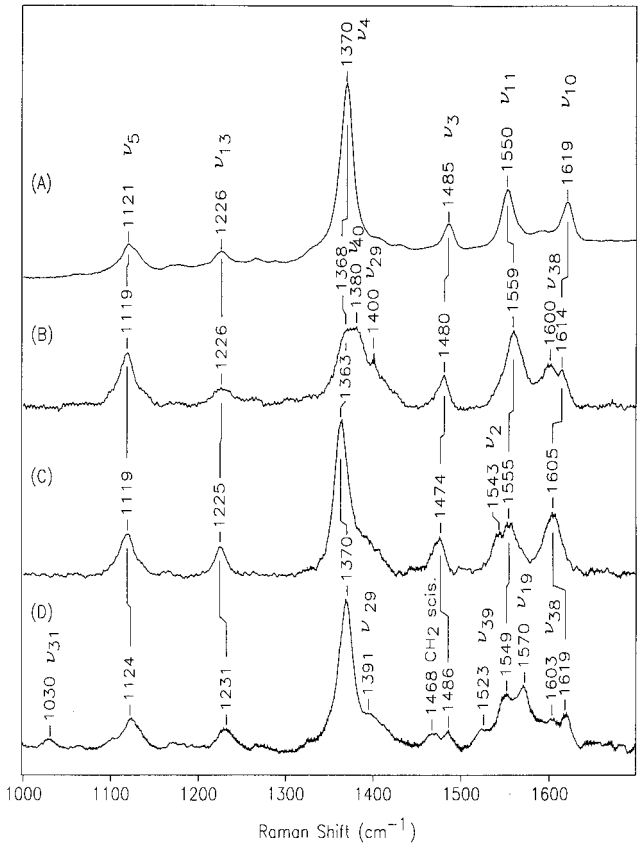

FIGURE 1: Resonance Raman spectra (1000−1700 cm^{-1}) of free base mesoporphyrin and *N*-methylmesoporphyrin using 406.7 nm excitation. (A) Aqueous free base mesoporphyrin IX (300 μM); (B) mesoporphyrin IX bound to the catalytic antibody (70μM); (C) aqueous *N*-methyl mesoporphyrin (300 μM); and (D) mesoporphyrin IX bound to ferrochelatase (55 μM) in the presence of Hg^{2+} (slight excess) (adapted from ref *16*). All solutions were maintained at pH 8.0 with Tris buffer. Band frequencies and assigned modes [based on NiOEP (*12*, *15*)] are indicated.

of enzyme-induced substrate distortion have also been noted in the literature (*4*).

Ferrochelatase catalyzes insertion of ferrous ions into protoporphyrin IX, and is essential for heme biosynthesis (*5*). In vitro, the enzyme has been found to accept other porphyrins such as mesoporphyrin IX and other divalent metal ions such as Zn(II) and Co(II) (*6*). However, still other metals, such as Mn(II), Cd(II), and Hg(II), are inhibitory (*7*). Ferrochelatase is also strongly inhibited by N-alkylated porphyrins (*8*), suggesting that the porphyrin distortion which is induced by N-alkylation serves to increase the rate of insertion. This is not unexpected, as it is known that N-alkylporphyrins chelate metal ions 3−5 orders of magnitude faster than nonalkylated porphyrins (*5*). This latter result is consistent with temperature jump experiments which provide an activation energy of approximately 7 kcal mol^{-1} to distort tetra(*N*-methylpyridyl)porphine (*10*). Antibodies raised to *N*-methylmesoporphyrin IX (N-MeMP)[1] have been found to catalyze insertion of Zn(II) and other divalent metal ions into mesoporphyrin free base (MPH_2) at rates of up to 10% of the enzymatic rate (*9*). As expected, the antibody reactivity is inhibited by the hapten.

[1] Abbreviations: N-MeMP, *N*-methylmesoporphyrin IX; MPH_2, mesoporphyrin free base; RR, resonance Raman; NiOEP, nickel octaethylporphyrin; Ab, antibody.

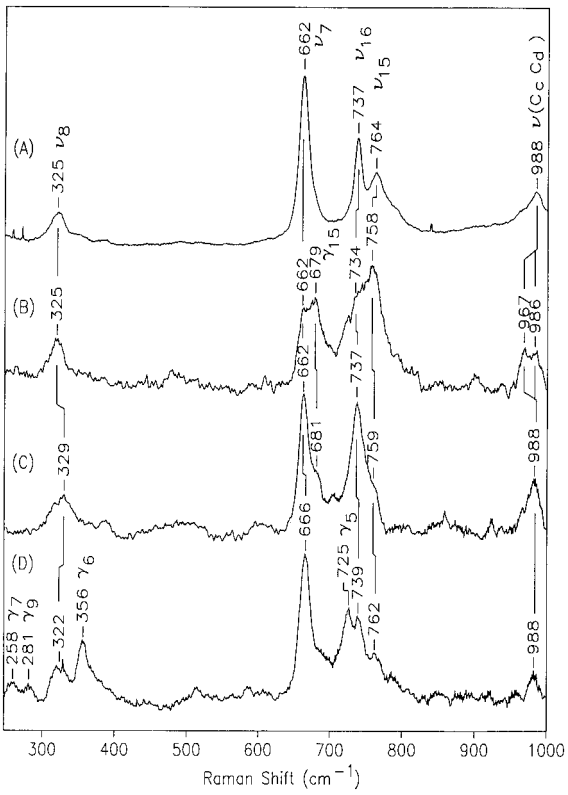

FIGURE 2: As Figure 1, but covering the low-frequency region (250−1000 cm^{-1}).

EXPERIMENTAL PROCEDURES

All porphyrins (N-MeMP and MPH_2) were obtained from Midcentury chemicals (Posen, IL). The preparation and purification of the antibody 7G12-A10-G1-A12 is described in detail elsewhere (*9*), as is the purification of yeast ferrochelatase (*11*). RR spectra were obtained by focusing 406.7 nm light from a Kr^+ laser (at an angle of 135°) onto spinning NMR tubes containing degassed samples. The scattered light was collected, *f*-matched, focused onto the slit of a triple grating monochromator, and detected with a diode array detector. Laser powers ranged from 8 to 25 mW, depending on the sample, and typical acquisition times were 10 min. The concentrations of the samples (in pH 8.0 Tris buffer) were as follows: (A) [MPH_2] = 300 μM, (B) [MPH_2] = 50 μM; [Ab] = 70 μM, (C) [N-MeMP] = 300 μM, and (D) [MPH_2] = 50 μM; [Fc] = 55 μM.

RESULTS

The high- and low-frequency RR spectra are shown in Figures 1 and 2, respectively. In the high-frequency region, several stretching vibrations of the ring CC and CN bonds were found to be shifted relative to the free MPH_2 solution spectra. Three of these modes (see ref *12* for the assignment scheme), ν_4 (1370 cm^{-1}), ν_3 (1485 cm^{-1}), and ν_{10} (1619 cm^{-1}) were found to be shifted down by 7−14 cm^{-1} for N-MeMP (spectrum C), while for antibody-bound MPH_2 (spectrum B), these same modes were also found to be shifted, but by smaller amounts (2−5 cm^{-1}). Additionally, the ν_{11} skeletal mode (1550 cm^{-1}) was found to be shifted up by 5 cm^{-1} in N-MeMP, and by even more in the bound MPH_2 spectrum (9 cm^{-1}). These shifts can be related to bonding changes observed in crystal structures of N-alkyl

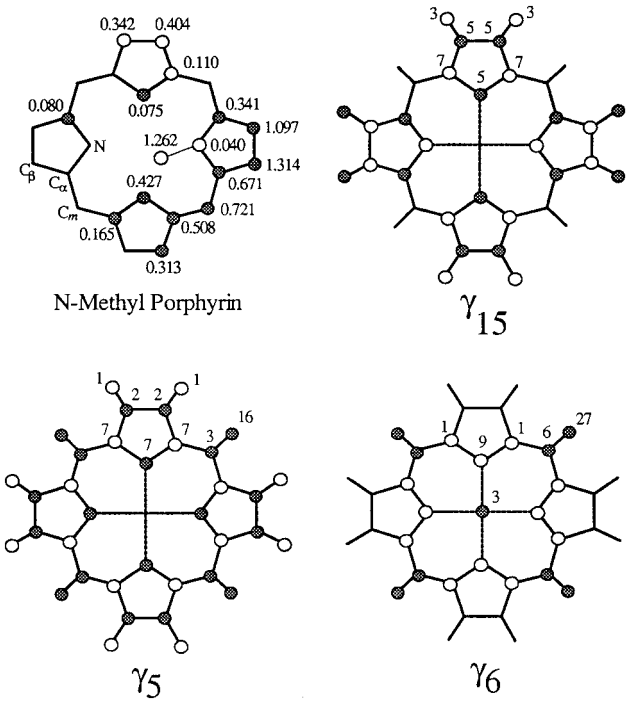

FIGURE 3: Structural diagram of a free base *N*-methylporphyrin (*13*) compared with the eigenvectors for γ_{15}, γ_5, and γ_6 (*15*). Atom labeling is indicated in the structural diagram, as well as the atomic displacements (in angstroms) from a plane defined by three of the C_m atoms. Open and filled circles in the eigenvector diagrams indicate the direction of the displacements of the atoms above and below the plane, while the numbers indicate their relative values.

porphyrins (*13*): the pyrrole ring bearing the N-alkyl group has slightly longer NC_α and $C_\beta C_\beta$ bonds, and slightly shorter $C_\alpha C_\beta$ bonds, than the nonalkylated pyrroles. This alternating pattern is reflected in the up- and downshifts of the skeletal modes, which contain variable contributions from the stretching of the pyrrole bonds (*12*). Some of the bonding effects are no doubt due to the direct electronic influence of the alkyl group, but additional effects may also arise from the out-of-plane distortion induced by the alkylation. As seen in Figure 3, this includes tilting of the pyrrole rings alternately above and below the mean porphyrin plane. Skeletal mode shifts that accompany out-of-plane porphyrin distortions have also been analyzed extensively by Shelnutt and co-workers (*14*). The fact that antibody-bound MPH_2 shows a similar pattern of frequency shifts, with no alkylation, strongly suggests that the out-of-plane distortion does affect bonding and that the distortion induced by the antibody resembles that induced by alkylation. In addition to frequency shifts, the out-of-plane distortion induces activity in modes which are inactive for aqueous MPH_2 because of the higher symmetry of the planar porphyrin; these include ν_{29}, ν_{38}, and ν_{40}.

The low-frequency spectrum (Figure 2) is even more revealing. Of particular significance is the activation of an out-of-plane vibration, γ_{15}, (see ref *15* for assignments) in both N-MeMP and antibody-bound MPH_2. The eigenvector of this mode [in the analogue NiOEP (*15*); Figure 3] shows it to involve alternating up and down displacements of the pyrrole N atoms. This is precisely the distortion pattern observed in N-alkylated porphyrins. Out-of-plane modes are unactivated in RR spectra of planar porphyrins (such as MPH_2), because there is no mechanism to couple them to

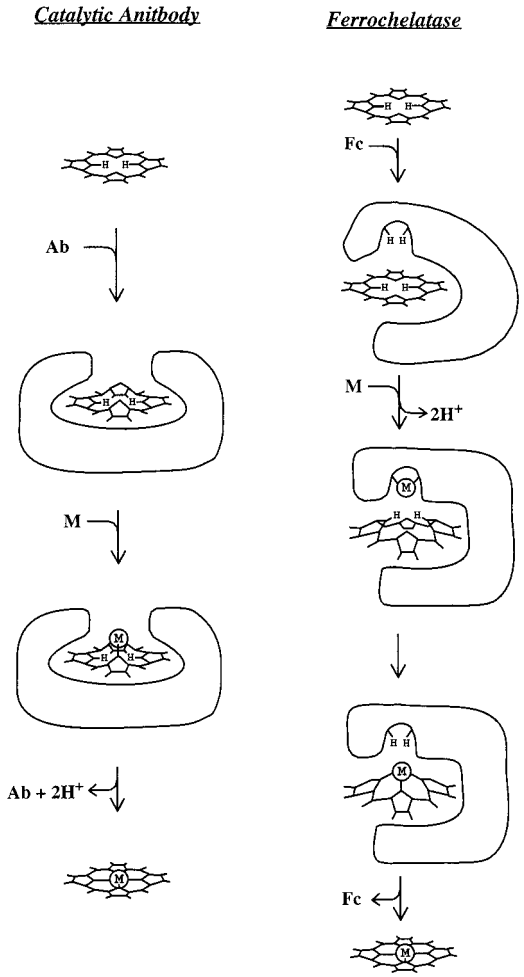

FIGURE 4: Model of the proposed mechanisms for metal insertion, highlighting the differences between ferrochelatase and the catalytic antibody. Although resonance Raman and fluorescence data show that porphyrin will bind in the abscence of metal (as shown here), kinetic data suggest that the metal actually binds before the porphyrin during catalysis.

the dominant in-plane electronic transition. However, an out-of-plane distortion renders one or more of the out-of-plane modes totally symmetric and, therefore, subject to resonance enhancement. The eigenvector of the vibration directly reflects the nature of the distortion. Thus, activation of γ_{15} is direct evidence that the catalytic antibody induces the same kind of distortion as does N-alkylation.

However, the ferrochelatase enzyme has a very different effect on the MPH_2 spectrum (*16*) than is found for the catalytic antibody. When MPH_2 is involved only in a binary complex with ferrochelatase, spectral changes are slight, reflecting little influence from the protein. However, when MPH_2 is involved in a ternary complex with ferrochelatase and the inhibitor Hg(II), the spectrum is markedly perturbed (spectrum D). These spectral changes are *not* observed for solutions containing only MPH_2 and Hg(II). In the ternary complex, extra bands are again activated in the high-frequency region (Figure 1), but no frequency shifts are observed for the skeletal modes. In the low-frequency region (Figure 2), out-of-plane modes are again enhanced, but they are *different* from those activated by N-alkylation. Especially prominent are γ_5 (725 cm^{-1}) and γ_6 (356 cm^{-1}). Their eigenvectors (*15*) (Figure 3) involve out-of-plane motions of all the N atoms in the *same* direction. Thus, the distortion

induced by ferrochelatase in the presence of added metal ion is a doming of the porphyrin [the lowest frequency mode of this symmetry type, γ_9, is exactly a doming motion of the entire porphyrin ring (*15*)] rather than an alternating up and down tilting of the pyrrole rings, as is observed in the N-alkyl porphyrin structures and the antibody-bound porphyrin].

DISCUSSION

It is not obvious which distortion, ruffling or doming, should better accommodate metal insertion nor is the detailed mechanism of the metal ligand exchange process well understood. In both cases, two pyrrole N sigma electron pairs become more accessible to the metal ion, while the two pyrroline protons, which must be displaced, become more exposed to solvent or a proton acceptor in the protein active site. Unfortunately, there are no domed metal-free porphyrin transition state models to test against N-MeMP. The fact that the reaction rate is within a factor of 10 between the antibody and the enzyme indicates that the distortions are comparable in their effectiveness.

However, enzyme and antibody differ in another respect: the former has a binding site for metal (*8*), whereas the latter does not. Saturation kinetics with respect to metal concentration is not observed for the antibody (*9*). Moreover, it is only when the site is occupied by an inhibitory metal (e.g., Hg^{2+}) that the enzyme-induced distortion of the porphyrin is observed. Thus, the antibody functions primarily through binding interactions with the porphyrin, whereas the enzyme must bind to both porphyrin and metal for catalysis. The latter interaction, which may involve a kinetically labile coordination complex with an active site residue such as a thiol (*5*), may account for the enhanced efficiency of the enzyme through a proximity effect (*17*). Moreover, metal-dependent distortion in the enzyme might be expected to provide a mechanism for enhanced metal ion specificity. In both the antibody and enzyme, metalation and the resulting planarization of the porphyrin ring might lead to decreased affinity for product. The observed product inhibition in the antibody-catalyzed reaction likely arises through axial ligation of the metalloporphyrin by a carboxylate side chain in the active site (R. Stevens, unpublished result). Thus, the antibody in many respects can be viewed as related to an ancestral porphyrin binding protein, which could either evolve as a ferrochelatase or oxygen binding/activating protein depending on the nature of metal ion complexation. Indeed the antibody has been shown to have a peroxidase activity (*18*).

Why, despite these mechanistic differences, does N-MeMP inhibit ferrochelatase? The answer probably lies in its positive charge, since N-MeMP is protonated at physiological pH (*19*). The metal binding site may contain an anionic ligand which could attract this positive charge. Cochran and Schultz (*9*) noted N-MeMP's charge equivalence with trivalent metal complexes [Fe(III) and Mn(III)] of mesoporphyrin, which markedly inhibit the catalytic antibody. However, these complexes are not distorted in a manner similar to N-alkyl porphyrins, but are instead somewhat domed. It appears that the exact shape of the porphyrin is less important for determining the strength of the binding interaction than is the charge, in both the catalytic antibody and the enzyme.

ACKNOWLEDGMENT

We would like to thank Harry A. Dailey for helpful discussions. T.S.R. would additionally like to acknowledge the National Institutes of Health for his postdoctoral fellowship.

REFERENCES

1. Haldane, J. B. S. (1930) in *Enzymes*, Longmans Green, London; Pauling, L. (1948) *Nature 161*, 707−709.
2. Tramontano, A., Janda, K. D., and Lerner, R. A. (1986) *Science 234*, 1566−1570; Pollack, S. J., Jacobs, J. W., and Schultz, P. G. (1986) *Science 234*, 1570−1573.
3. Schultz, P. G., and Lerner, R. A. (1995) *Science 269*, 1835−1842; Schultz, P. G., Lerner, R. A., and Benkovic, S. J. (1990) *Chem. Eng. News 68*, 26−40; Schultz, P. G. (1989) *Acc. Chem. Res. 22*, 287−294; Schultz, P. G. (1989) *Angew. Chem., Int. Ed. Engl. 28*, 1283−1295.
4. Belasco, J. G., and Knowles, J. R. (1980) *Biochemistry 19*, 472−477; Harrison, R. K., and Sterin, R. L. (1990) *Biochemistry 29*, 1684−1689; Komives, E. A., Chang, L. C., Lolis, E., Tilton, R. F., Petsko, G. A., and Knowles, J. R. (1991) *Biochemistry 30*, 3011−3019; Lodi, P. J., and Knowles, J. R. (1991) *Biochemistry 30*, 6948−6956.
5. Lavallee, D. K. (1988) *Mol. Struct. Energ. 9*, 279−314.
6. Dailey, H. A., Jones, C. S., and Karr, S. W. (1989) *Biochim. Biophys. Acta 999*, 7−11; Li, F. M., Lim, C. K., and Peters, T. J. (1987) *Biomed. Chromatogr. 2*, 164−168; Roberts, R. G. (1987) *Biomed. Chromatogr. 2*, 71−75; Rossi, E., Costin, K. A., and Garcia-Webb, P. (1988) *Clin. Chem. 34*, 2481−2485.
7. Dailey, H. A. (1990) in *Biosynthesis of Heme and Chlorophylls*, (Dailey, H. A. Ed.) McGraw-Hill Publishing, New York.
8. Dailey, H. A., and Fleming, J. E. (1983) *J. Biol. Chem. 258*, 11453−11459.
9. Cochran, A. G., and Schultz, P. G. (1990) *Science 249*, 781−783.
10. Pasternack, R. F., Sutin, N., and Turner, D. H. (1976) *J. Am. Chem. Soc. 98*, 1908.
11. Sellers, V. M., and Dailey, H. A. (1997) *Methods Enzymol. 281*, 378−387.
12. Li, X.-Y., Czernuszewicz, R. S., Kincaid, J. R., Stein, P., and Spiro, T. G. (1990) *J. Phys. Chem. 94*, 1990, 47−61.
13. Lavallee, D. K., and Anderson, O. P. (1982) *J. Am. Chem. Soc. 104*, 4707−4708.
14. Jentzen, W., Song, X.-Z., and Shelnutt, J. A. (1997) *J. Phys. Chem. B 101*, 1684−1699.; Song, X.-Z., Jentzen, W., Jia, S.-L., Jaquinod, L., Nurco, D. J., Medforth, C. J., Smith, K. M., and Shelnutt, J. A. (1996) *J. Am. Chem. Soc. 118*, 12975−12988.; Jentzen, W., Simpson, M. C., Hobbs, J. D., Song, X., Ema, T., Nelson, N. Y., Medforth, C. J., Smith, K. M., Veyrat, M., Mazzanti, M., Ramasseul, R., Marchon, J.-C., Takeuchi, T., Goddard, W. A., III, and Shelnutt, J. A. (1995) *J. Am. Chem. Soc. 117*, 11085−11097.
15. Li, X.-Y., Czernuszewicz, R. S., Kincaid, J. R., and Spiro, T. G. (1989) *J. Am. Chem. Soc. 111*, 7012−7023.
16. Blackwood Jr., M. E., Rush, T. S., III, Medlock, A., Dailey, H. A., and Spiro, T. G. (1997) *J. Am. Chem. Soc.* (in press).
17. Page, M. I., and Jencks, W. P. (1971) *Proc. Natl. Acad. Sci. U.S.A. 68*, 1678−1683.
18. Cochran, A. G., and Schultz, P. G. (1990) *J. Am. Chem. Soc. 112*, 9414−9415.
19. Lavallee, D. K. (1988) in *The Chemistry and Biochemistry of N-Substituted Porphyrins*, VCH, New York.

BI972616F